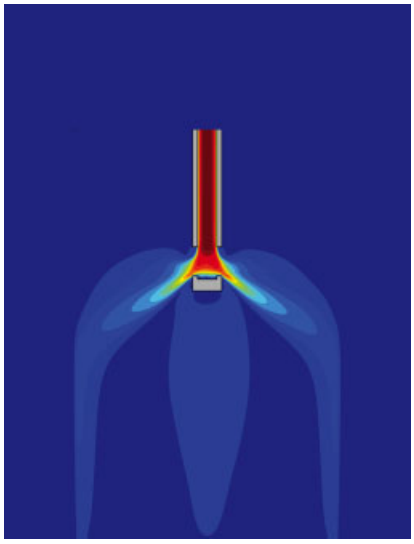

steel research international

www.steel-research.de

Cover Photo:

The figure shows the contour plot of the time averaged velocity field in the mini-LIMMCAST mold model. Results are calculated by unsteady RANS simulations. Despite the symmetrical pattern shown in this figure, the study reveals that strong deviations can occur due to choice of the turbulence model and order of discretization in such kind of flows.

Publishing company:

Wiley-VCH Verlag GmbH & Co. KGaA, Boschstraße 12, D-69469 Weinheim, Germany

Contents

The paper deals with a mathematical model of counter-current flow in a blast furnace for a complex evaluation of iron-ore bearing raw materials reducibility. It is based on laboratory tests results and model calculation to predict the parameters of the reduction process and specific consumption of carbon in the blast furnace by Rist.

Contents

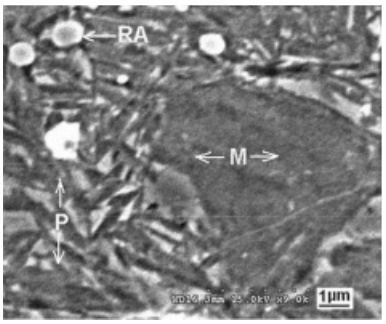

The cooling curves are generated for 1080 steel through explicit finite difference based model considering constant values of thermal conductivity and specific heat. Grange–Kiefer approach is extended for determination of 50% transformation nose of CCT diagram. The cooling curves are solved against 50% transformation nose of CCT diagram. The D_u/D versus D plots are generated for both finite and infinite severity of quenchant. The D_C predicted by the model closely matches with the experimental D_C.

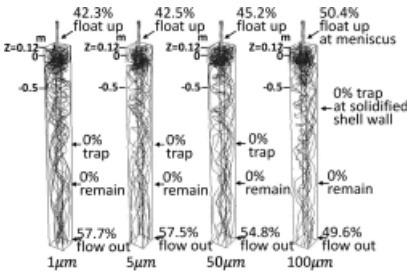

It can be seen in a no-swirl flow case that the inclusions are concentrated in the upper part of a mold, which consists of the meniscus/stagnant region (from Z=0.12 to− 0.3 m) and the circulation flow region (from Z=−0.3 to −1.1 m). However, it is found for a swirl flow case that the inclusions are concentrated in the upper part of a mold, which consists of the meniscus region (from Z=0.12 to 0.05 m) and the circulation flow region (from Z=0.05 to −0.5 m). Moreover, all inclusions are more easily removed to a meniscus for a swirl-flow case than for a no-swirl flow case.

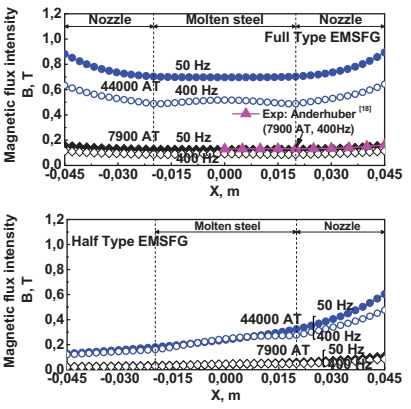

Two kinds of a full type and a half type electromagnetic swirl flow generators (EMSFG) are studied. Moreover, those two type devices with different magnetomotive forces, frequencies as well as core distances are also investigated. Furthermore, the distribution of the magnetic flux intensity in molten steel and EMSFG and the distribution of the Lorentz force in molten steel are discussed by using different EMSFG structures and electromagnetic parameters.

Contents

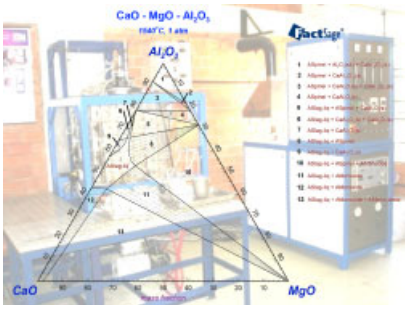

In the production of special steels, inclusions have a significant influence on final product quality. The main objective of this study is to conduct a thermodynamic study aimed at preventing clogging problems during continuous casting (CC) and the formation of undesirable inclusions. Alumina (Al_2O_3), spinels, and calcium sulfide (CaS) are potential sources of defects during rolling and steel forging.

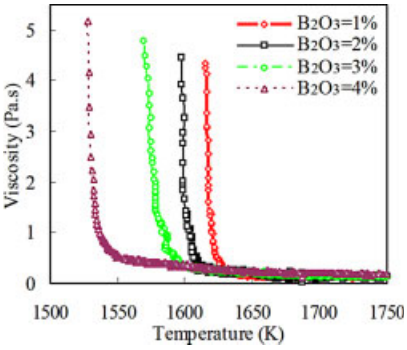

All the viscosities are within 0.2 Pas for high temperature (over 1633 K in this experiment), which is less than that of the B-free slag. However, the value increases sharply when temperature is below break point temperature. In addition, an increase in the value of B_2O_3 content reduces significantly break point temperature and descent rate of temperature rises with increasing B_2O_3 content.

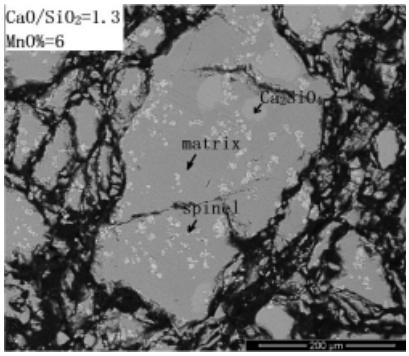

Manganese is found to be enriched in spinel and liquid. The spinel increases in size with increasing of MnO and decreasing of CaO/SiO_2 ratio. Disintegration is found in samples with increased MnO content and CaO/SiO_2 ratio, which can be interpreted by increase of the size of Ca_2SiO_4 with increase of MnO content and CaO/SiO_2 ratio.

A time resolving numerical model of a single-phase mold is formulated in the frame of Reynolds-averaged Navier–Stokes (RANS) simulations. Thereby the performance of various turbulence models is evaluated focusing the jet flow. The results show, that it is necessary to have higher order discretization with either the RNG k–ε model or the k–ω SST model.

Contents

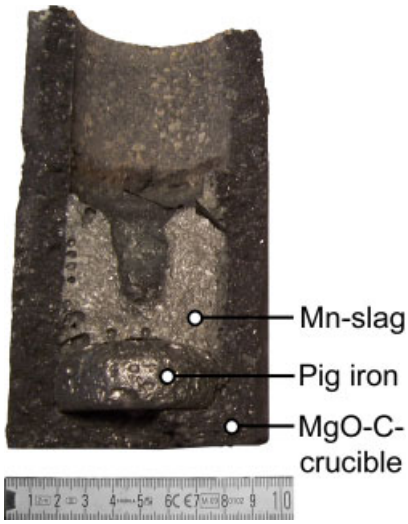

Concerning the industrial production of high manganese steel melts, conventional Mn-bearing alloying agents are reviewed. A modified process route for pyrometallurgical winning of special silicomanganese grades tailored for high manganese steelmaking is conceived. For each individual process step, namely manganese slag production, silicomanganese production, and optional desiliconization of silicomanganese, results of lab-scale experiments are discussed.

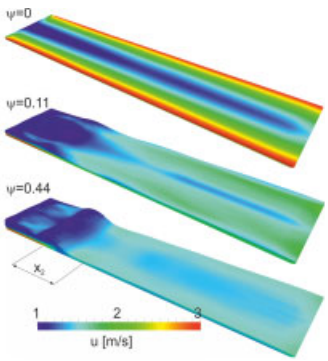

Visualization of the computed free surface flow with inflow disturbances for different magnetic fields imposed in the marked region. The color represents the magnitude of velocity.

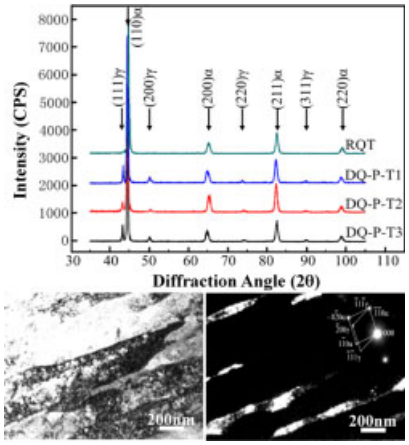

A novel direct quenching–partioning– tempering (DQ–P–T) process is presented and applied to a low-alloy Mn–Si–Cr cast steel. DQ–P–T cast steels have higher volume fractions of the retained austenite than traditional reheat quenching and tempering (RQT) steel, and show the improved microstructure consisting of the dislocation-type lath martensite and nano-sized flake-like retained austenite between martensite laths, which results in enhanced mechanical properties of the cast steel.

steel research international

Contents

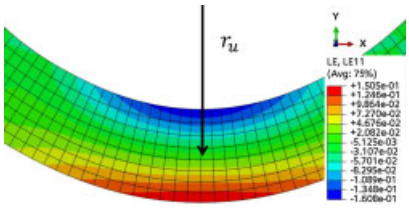

Especially in roll-forming, designers are still challenged by determining the initial sheet width, since many different approaches exist for this calculation leading to different results. This article compares different experimental approaches to determine the initial sheet width and provides a starting point for further studies to improve the calculation methods.